K-EDGE CODED APERTURES FOR COMPRESSIVE SPECTRAL X-RAY TOMOGRAPHY

Angela P. Cuadros [1], *Xu Ma* [2] *and Gonzalo R. Arce* [1] *

[1] Department of Electrical and Computer Engineering, University of Delaware, Newark, DE 19716
[2] School of Optics and Photonics, Beijing Institute of Technology, Beijing, 100081, China

ABSTRACT

Spectral computed tomography (SCT) is used to perform material characterization in 3D images, a feature that is not possible with conventional computed tomography (CT) systems. Currently, photon-counting detectors are used to obtain the energy binned images in SCT, however, these detectors are costly and the measured data have low signal to noise ratios. This paper presents a new approach for SCT which circumvents the limitations of current SCT systems. It combines conventional X-ray imaging systems with K-edge coded aperture masks. In this scheme, a particular filter pair is aligned with each X-ray beam in a multi-shot architecture, therefore obtaining compressive measurements in both the spectral and spatial domains. Then, the energy binned images are reconstructed using the alternating direction method of multipliers (ADMM) to solve a joint sparse and low-rank optimization problem that exploits the structure of the spectral data-cube. Simulations using coded fan-beam X-ray projections demonstrate the feasibility of the proposed approach.

Index Terms— X-ray imaging, compressive sensing, spectral CT, K-edge filters, coded apertures.

1. INTRODUCTION

Tomographic grayscale images are insufficient to reveal differences between materials having different chemical composition but the same X-ray attenuation coefficient for a particular X-ray energy. Spectral X-ray information reveals the energy-dependent attenuation properties of the object and allows material identification [1]. Thus, recently there has been growing interest in spectral computed tomography (SCT) techniques which aim at revealing material characterization of an object by using information from all of the X-ray spectra [2, 3]. Photon counting detectors are usually used for SCT, as they are able to obtain attenuation data from multiple energy bins, therefore allowing various materials to be distinguished in a single acquisition [4]. However, such detectors are prohibitively costly for some applications, and the measured data have low signal to noise ratios (SNR) due to the detector's narrow bin bandwidth and quantum noise [5]. Furthermore, the complexity of the sensor layers limits the resolution of the detectors, which is compromised when more energy bins are needed [6]. Rakvongthai et al. proposed an SCT system which used different K-edge filters in sequential CT scans to obtain mono-energetic X-ray flux data [7]. This architecture overcomes the photon counting detectors limitations; however, the acquisition time and radiation dose are higher given that a complete scan is needed for each K-edge filter used.

This paper presents a new approach for SCT that uses K-edge coded apertures in conjunction with conventional X-ray imaging systems to obtain spatially and spectrally coded illumination projections of the object. The proposed system uses two or more shots in which the pixels of the coded apertures are chosen from a set of balanced K-edge filters, such that a particular pair is assigned to a particular detector position as shown in Fig. 1(a). In this way, by subtracting the filtered measurements, quasi-monochromatic sinograms can be obtained at the energy bins described by the balanced K-edge filters, as proposed by Ross [8, 9]. The resulting sinograms, however, are highly under-sampled since only a subset of the detectors is paired with a certain balanced pair. Thus, the alternating direction method of multipliers (ADMM) is used to solve the highly ill-posed problem by exploiting the inherent sparsity of X-ray images in the spatial domain and the low-rank structure of the data-cube [10]. This paper demonstrates the feasibility of the new SCT approach by studying the performance in a fan-beam setting. Simulations show that the radiation dose and scanning time can be reduced significantly while maintaining the reconstruction quality.

2. K-EDGE SCT FORWARD MODEL

When a filter f is placed in front of an X-ray source, the intensity of an X-ray beam at the energy E after passing through the filter is given by $I_f(E) = I_0(E)\exp[-\mu_f(E)\delta_{j,f}]$, where $\mu_f(E)$ is the linear attenuation coefficient of the filter f at the energy E, and $\delta_{j,f}$ is the length of the intersection of the j^{th} X-ray beam with the filter f [11]. The latter is given by $\delta_{j,f} = \rho_f/\cos(\psi_j)$, where ρ_f is the thickness of the filter and ψ_j is the angle between the normal of the filter and the j^{th} X-ray beam. Thus, the filtered measurements on the j^{th}

*This work was supported in part by the National Science Foundation (NSF) under Grant CIF 1717578 and an University of Delaware UNIDEL Grant.

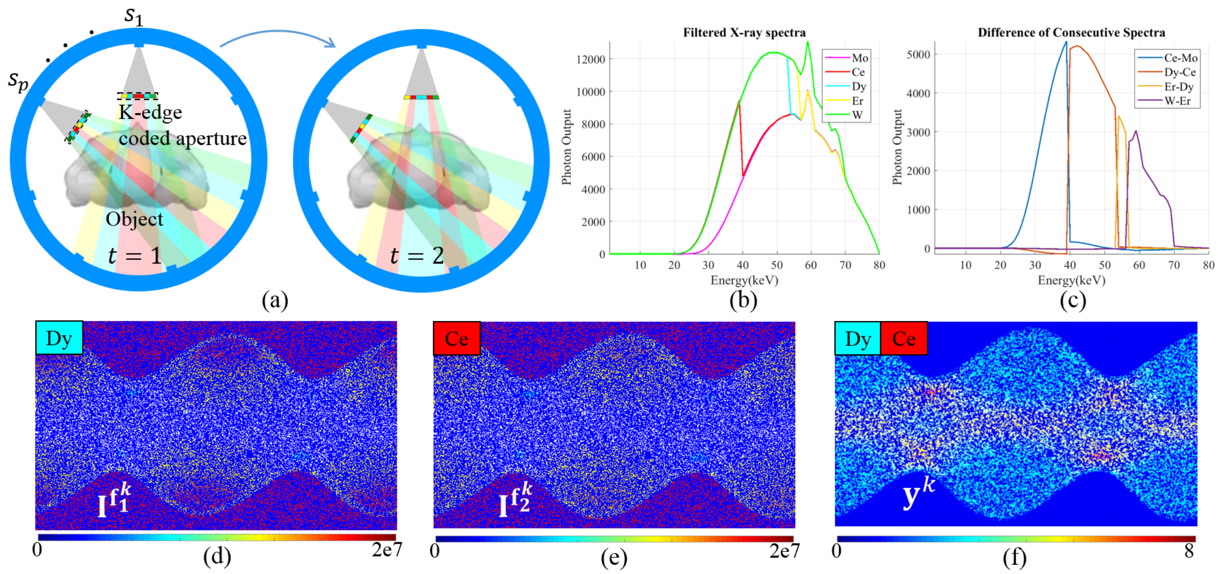

Fig. 1. (a) K-edge coded aperture system for compressive spectral X-ray fan-beam CT for $T = 2$ shots. Different coded apertures are placed in front of the rotating source for each location s_p. (b) Energy spectra of an 80 keV X-ray source seen through the five different filters used in the K-edge coded aperture mask (Mo, Ce, Dy, Er, and W). (c) Quasi-monochromatic energy-binned spectra obtained using the corresponding pairs. Filtered measurements acquired using Dy, (d) $I^{f_1^k}$, and Ce, (e) $I^{f_2^k}$. (f) Log-normalized sinogram $\mathbf{y}^k$ at the $k = 2$ energy bin.

element using an integrating detector are given by:

$$I_j^f = \int_E I_f(E) \exp(-\int_\ell \mu(\ell, E) d\ell) dE. \qquad (1)$$

If P is the total number of X-ray source positions and M is the number of detector elements in the detector array, then $j = 1, \ldots, MP$. The integrated grayscale data in (1) cannot be used to reconstruct directly the energy-binned images $\mu(\ell, E)$, as it does not provide spectrally resolved data [12]. Photon counting detectors and monochromatic synchrotron X-ray sources are able to provide such energy selective measurements; however, these devices are costly and not easily accessible. A cost-effective alternative to obtain quasi-monochromatic X-ray spectra are Ross filter pairs [13,14]. In principle, Ross filters produce a monochromatic effect by using two balanced filters that consist of materials with nearly adjacent atomic numbers whose thicknesses are matched such that the transmitted spectra are identical for all photon energies except in the narrow energy bin between their respective K-edges [8,15]. The quasi-monochromatic measurements are then obtained by subtracting the X-ray intensity acquired using the filter with the lower K-edge from that with the higher K-edge in the Ross pair [13]. Therefore, the bandwidth of the energy bin is defined by the difference between the K-edge energies of the two elements constituting the Ross pair. Figure 1(b) depicts the energy spectra of a simulated 80 kV X-ray source seen through the five different filters and Fig. 1(c) depicts the spectra of the energy bins obtained using the Ross filter pairs.

The proposed system uses coded apertures with multiple material filters to obtain spatially and spectrally coded illumination projections of the object, thus the name K-edge coded apertures. Different coded aperture patterns are used for each view angle position s_p, where $p = 1, \ldots, P$, and each shot t where $t = 1, \ldots, T$ as shown in Fig. 1(a), which depicts the proposed system for a fan beam architecture with $T = 2$ shots. As previously mentioned, the measurements obtained by a single scan are not sufficient when using the Ross filter method. Thus, it is necessary to perform a second scan in which the corresponding Ross pair is assigned to each detector position j. In this way, in the first shot $t = 1$, the K-edge coded aperture contains one of the materials of the pair in the position j and in the second shot, $t = 2$, the coded aperture contains the other material from the pair in the same position, as shown in Fig. 1(a). Using these measurements, the quasi-monochromatic intensity at the k^{th} energy bin at the j^{th} detector element can be obtained as $d_j^k = I_j^{f_1^k} - {}_j^{f_2^k}$, where $I_j^{f_1^k}$ and $I_j^{f_2^k}$ are the measurements taken by the filters with higher and lower K-edges in the Ross pair associated with the k^{th} energy bin, respectively. The discretized set of measurements, referred to as the sinogram, corresponds in each case to the measurements of the detectors paired with the respective filter. Figures 1(d)-1(e) depict the measurements obtained using Dysprosium (Dy) and Cerium (Ce), that is $\mathbf{I}^{f_1^k} = [I_1^{f_1^k}, \ldots, I_{MP}^{f_1^k}]^T$ and $\mathbf{I}^{f_2^k} = [I_1^{f_2^k}, \ldots, I_{MP}^{f_2^k}]^T$, respectively. Note both sinograms contain information in the same

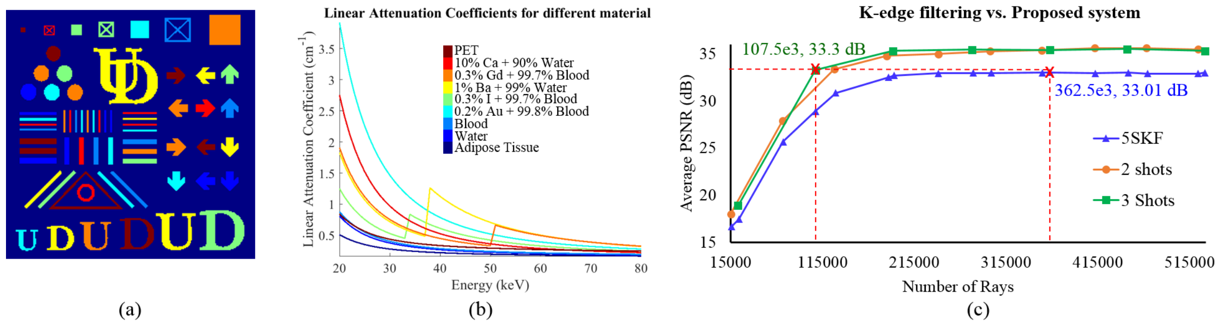

Fig. 2. (a) Simulated phantom and (b) corresponding linear attenuation coefficients with respect to the energy. (c) Average PSNR for the 5SKF and the proposed system for 2 shots and 3 shots for different numbers of rays.

location such that the filtered measurements can be subtracted to obtain the quasi-monochromatic intensities d_j^k. Recall, from the Beer-Lambert law $d_j^k = d_{j0}^k \exp\left[-\int_\ell \mu(\ell,k)d\ell\right]$ where d_{j0}^k is the quasi-monochromatic intensity, and $\mu(\ell,k)$ is the linear attenuation coefficient at the k^{th} energy bin. Then, the log-transformed measurements can be obtained as $y_j^k = \ln(d_{j0}^k)/(d_j^k)$ for the k^{th} energy bin associated with the Ross filter pair assigned to the position j. Note $y_j^m = 0$, whenever $m \neq k$. Figure 1(f) depicts the final log-normalized energy binned sinogram for $k = 2$. Discretizing the line integrals and the linear attenuation coefficients $\mu(\ell,k)$, the energy-binned measurements $\mathbf{y}^k = [y_1^k, y_2^k, \ldots, y_{MP}^k]^T$ are given by the following linear model

$$\mathbf{y}^k = \mathbf{C}^k\mathbf{H}\mathbf{x}^k, \tag{2}$$

where $\mathbf{x}^k \in \mathbb{R}^{N^2\times 1}$ is the vectorized linear attenuation coefficient $\mu(\ell,k)$ of the $N \times N$ discretized object under inspection at the k^{th} energy bin, $\mathbf{H} \in \mathbb{R}^{MP\times N^2}$ is the CT system matrix such that the weights $\mathbf{H}_{j,i}$ account for the hardware settings, and $\mathbf{C}^k$ is the coded aperture matrix. Each row of the matrix, $\mathbf{H}$, corresponds to a particular detector element j, and each detector is associated with a particular Ross filter pair which in turn is associated with a particular energy bin k. Thus, the elements of the coded aperture matrix $\mathbf{C}^k$ select the rows of the matrix $\mathbf{H}$ associated with the Ross filter pair that corresponds to the k^{th} energy bin. Mathematically, the coded aperture matrix $\mathbf{C}^k$ is defined as a diagonal binary matrix, where $\mathbf{C}_{j,l}^k = 0$ for $j \neq l$, and $\mathbf{C}_{j,j}^k = 1$ if the K-edge coded aperture element associated with the j^{th} detector contains the elements of the Ross filter pair corresponding to the k^{th} energy bin, otherwise $\mathbf{C}_{j,j}^k = 0$. Ross filter pairs are assigned randomly to each detector element j following a uniform distribution; as a result, the number of measurements per energy bin is given by $D = MP/K$, where K is the total number of energy bins. The reconstruction of each energy bin is thus a highly ill-posed problem. Hence, to effectively recover the object from the compressed measurements, regularization constraints are added based on the structure of the data. In this paper, a joint sparse and low-rank optimization method is used. This approach seeks to jointly minimize the ℓ_1 norm of the sparse representation of the data cube, and its nuclear norm. Furthermore, the tensor modeling previously proposed for SCT in [6] and [16] is used to formulate the reconstruction problem as: argmin $\frac{1}{2}||\mathcal{Y} - \mathcal{A}(\mathcal{X})||_2^2 + \eta_1||\text{vec}(\Psi(\mathcal{X}))||_1 + \eta_*||\mathcal{X}||_*$, where $\mathcal{X} \in \mathbb{R}^{N\times N\times K}$ is a tensor concatenating the energy-binned images $\mathbf{x}^k$, $\mathcal{Y}$ is the vertical concatenation of the quasi-monochromatic sinograms $\mathbf{y}^k$, $\mathcal{A}(*)$ is the tensor expression used to generalize the forward projection in (2) for $k = 1, \ldots, K$, Ψ is a sparsifying basis, η_1 and η_* are regularization constants, and $\text{vec}(\mathcal{X}) = \left[\mathbf{x}^{1\,\text{T}}|\mathbf{x}^{2\,\text{T}}|\ldots|\mathbf{x}^{K\,\text{T}}\right]^T$. The ADMM algorithm [17] is adapted to solve the inverse problem as it provides the necessary tools to split the optimization problem into small convex optimization problems that can be solved using simpler algorithms.

3. SIMULATION RESULTS

A simulation experiment for an X-ray fan beam system with K-edge coded apertures is performed using a 256×256 simulated phantom (Fig. 2(a)). The number of detector elements per view was set to $M = 512$, the source to detector distance and the source to object distance was set 80 cm and 40 cm respectively and the detector length was set to 41.3 cm. The phantom consists of nine different materials which linear attenuation coefficients are depicted in Fig. 2(b). These linear attenuation coefficients were obtained from the National Institute of Standards and Technology (NIST) X-ray attenuation databases available in [18]. The X-ray filtered spectra $I_f(E)$ were simulated at 80 keV using the Spektr software [19] and energy weighted integrals over 1keV spectral steps were obtained for each filtered measurement according to (1). The projection data were simulated using the ASTRA tomography toolbox [20]. A copper (Cu) filter of 0.25 mm was placed in front of the X-ray source to filter the energies lower than 20 kV. After matching the Ross filter pairs [13], the thickness of the Molybdenum (Mo), Cerium (Ce), Dysprosium (Dy), Erbium (Er), and Tungsten (W) filters were set to be 74.7, 52.8, 30.6, 26.7 and 9.9 μm respectively. The filter pairs assigned

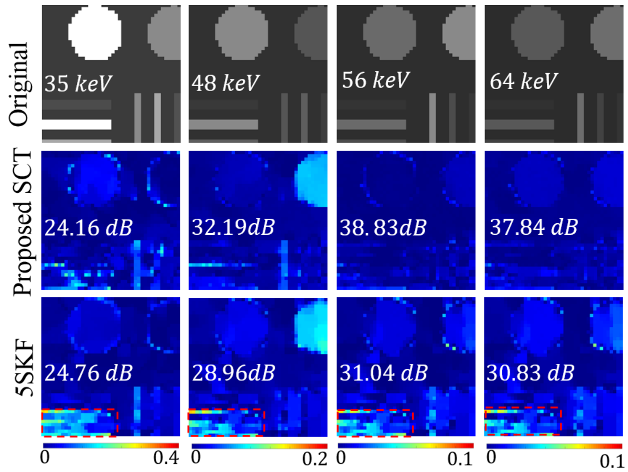

Fig. 3. The zoomed version of the original images (top) and the corresponding absolute reconstruction errors by the proposed system for 3 shots (middle) and the 5SKF system (bottom) for each energy k.

to each detector position j were chosen randomly from Ce-Mo [20.0-40.4 keV], Dy-Ce [40.4-53.8 keV], Er-Dy [40.4-53.8 keV] and W-Er [57.5-69.5 keV]. That is if Er-Dy was assigned to the detector position $j = 1$, then in the first scan, the K-edge coded aperture contained Er at the position $j = 1$ and in the second scan it contained Dy at the same position. To evaluate the performance of the proposed system, reconstructions using the system developed by Rakvongthai et al. in [7] (hereafter referred to as 5 Shot K-edge filtering (5SKF)) are performed and compared with the proposed model. The radiation dose is set to be equivalent in both systems; that is, the number of measurements acquired with each filter is set to be the same in each case. In the ADMM algorithm, the energy-binned CT image is represented using a Kronecker product between the discrete cosine transform (DCT) basis and the 2D Haar wavelet basis [21]. The reconstructions of both systems are compared to the linear attenuation images, obtained from the NIST database, corresponding to the central energy in each energy bin, that is, 35 keV for $k = 1$, 48 keV for $k = 2$, 56 keV for $k = 3$, and 64 keV for $k = 4$. The peak signal to noise ratio (PSNR) is used to evaluate the reconstructions since it is suitable for comparing restoration results [22].

Some filter elements are used to obtain more than one energy binned sinogram. Here, for example, Ce is used for both $k = 1$ and $k = 2$, Dy is used for both $k = 2$ and $k = 3$, and Er is used for both $k = 3$ and $k = 4$. Thus, for a system with $T > 2$ shots, instead of selecting a particular filter pair for each detector position j, a trio of elements can be assigned, such that one of the elements of the trio is used in more than one energy bin. This trio assignment can increase the number of samples in the subsampled sinograms, thus retaining more spectral information for each energy bin and improving the reconstruction performance especially when a large number of filters are used. For $T = 3$, the elements of the K-edge coded apertures were chosen from Mo-Ce-Dy and Dy-Er-W for each detector position j which resulted in energy-binned sinograms with 50% sub-sampling. In this work, the reconstructions of the 5SKF system were performed using total variation (TV) regularization to exploit the sparsity of the object and counteract the limited view angle problem in low-dose scenarios. Figure 2(c) shows the average PSNR of the energy-binned reconstructions from the proposed system for 2 and 3 shots, as well as the 5SKF systems for different P values. It should be noted that the average PSNR of the reconstructions obtained with the proposed system is higher for all the view angles for both $T = 2$ and $T = 3$ compared to the 5SKF system. Additionally, the radiation dose required by the proposed system to obtain an average PSNR of 33.3 dB is approximately 30% of the radiation dose necessary in the 5SKF system to obtain a similar performance, which is of interest in medical applications. Image reconstruction errors for the four energy bins and a zoomed portion of the figure are shown for the proposed system for $T = 3$ and the 5SKF system in Fig. 3. The first row corresponds to the original images, and the second and third rows correspond to the absolute error of the reconstructions using the proposed system with 3 shots and the 5SKF system, respectively. As it can be seen, there are more artifacts in the reconstructions obtained using the 5SKF system compared to the proposed system even when using sparsity regularization constraints for both reconstructions. Furthermore, the PSNR improvement is up to 7 dB in the third and fourth energy bins.

4. CONCLUSION AND FUTURE WORK

A spectral computed tomography system which uses conventional X-ray imaging systems combined with a set of K-edge coded aperture filters is proposed. It has the potential to provide a cost-effective alternative to photon counting SCT techniques and a faster scanning solution with reduced X-ray radiation dose compared to the traditional K-edge filter scanning proposed in [7]. Simulations showed an improvement of up to 7 dB in the reconstructions using the proposed system compared to the 5SKF system. Moreover, the reconstructions obtained with the proposed system exhibited better quality at lower X-ray radiation dose. Particularly, simulations show that the 3 shot system is able to attain reconstructions of 33.3 dB average PSNR with 70% less of the radiation than the 5SKF system. The proposed system can be extended to distinct sets of Ross filters to obtain more energy bins and this is a topic of current work. This paper uses coded apertures generated randomly, however, techniques to optimize the number of energy bins and the distribution of the Ross filters are a topic of future work. Furthermore, experimental fabrication of the coded apertures and experimental reconstructions are being developed.

5. REFERENCES

[1] B. J. Heismann, B. T. Schmidt, and T. G. Flohr, *Spectral Computed Tomography*, SPIE Press Book, 2012.

[2] J. Hsieh, N. Chandra, S. Woloschek, B. Senzig, S. Aluri, T. Benson, X. Wu, D. Okerlund, and B. Li, "CT spectral projection imaging," in *2009 IEEE Nuclear Science Symposium Conf. Record*, Oct 2009, pp. 3513–3516.

[3] J P Schlomka, E Roessl, R Dorscheid, S Dill, G Martens, T Istel, C Baumer, C Herrmann, R Steadman, G Zeitler, A Livne, and R Proksa, "Experimental feasibility of multi-energy photon-counting K-edge imaging in pre-clinical computed tomography," *Physics in Medicine and Biology*, vol. 53, no. 15, pp. 4031, 2008.

[4] I. Glass, A. P. H. Butler, P. H. Butler, P. J. Bones, and S. J. Weddell, "Physiological gating of the MARS spectral micro CT scanner," in *28th Int. Conf. on Image and Vision Computing New Zealand (IVCNZ)*, 2013, pp. 317–322.

[5] K. Taguchi, M. Zhang, E. C. Frey, X. Wang, J. S. Iwanczyk, E. Nygard, N. E. Hartsough, B. M. W. Tsui, and W. C. Barber, "Modeling the performance of a photon counting X-ray detector for CT: Energy response and pulse pileup effects," *Medical Physics*, vol. 38, no. 2, pp. 1089–1102, 2011.

[6] L. Li, Z. Chen, W. Cong, and G. Wang, "Spectral CT modeling and reconstruction with hybrid detectors in dynamic-threshold-based counting and integrating modes," *IEEE Trans. on Medical Imaging*, vol. 34, no. 3, pp. 716–728, March 2015.

[7] Y. Rakvongthai, W. Worstell, G. El Fakhri, J. Bian, A. Lorsakul, and J. Ouyang, "Spectral CT using multiple balanced K-edge filters," *IEEE Trans. on Medical Imaging*, vol. 34, no. 3, pp. 740–747, March 2015.

[8] P. Ross, "Polarization of X-rays," *Phys. Rev*, vol. 28, pp. 425, 1926.

[9] P. A. Ross, "Polarization of X-rays from a tungsten target," *J. Opt. Soc. Am.*, vol. 16, no. 6, pp. 375–379, Jun 1928.

[10] H. Gao, H. Yu, S. Osher, and G. Wang, "Multi-energy CT based on a prior rank, intensity and sparsity model (PRISM)," *Inverse Problems*, vol. 27, no. 11, pp. 115012, 2011.

[11] J.L. Prince and J.M. Links, *Medical imaging signals and systems*, Pearson Prentice Hall, 2006.

[12] J. Chu, W. Cong, L. Li, and G. Wang, "Combination of current-integrating and photon-counting detector modules for spectral CT," *Physics in Medicine and Biology*, vol. 58, no. 19, pp. 7009, 2013.

[13] M. Saito, "Quasimonochromatic X-ray computed tomography by the balanced filter method using a conventional X-ray source," *Medical Physics*, vol. 31, no. 12, pp. 3436–3443, 2004.

[14] B. D. Arhatari and T. E. Gureyev, "Elemental contrast X-ray tomography using Ross filter pairs with a polychromatic laboratory source," *Scientific Reports*, vol. 7, no. 1, March 2017.

[15] P. Kirkpatrick, "On the theory and use of Ross filters," *Review of Scientific Instruments*, vol. 10, no. 6, pp. 186–191, 1939.

[16] L. Li, Z. Chen, G. Wang, J. Chu, and H. Gao, "A tensor PRISM algorithm for multi-energy CT reconstruction and comparative studies," *Journal of X-Ray Science and Technology*, vol. 22, no. 2, pp. 147–163, 2014.

[17] S. Boyd, N. Parikh, E. Chu, B. Peleato, and J. Eckstein, "Distributed optimization and statistical learning via the alternating direction method of multipliers," *Found. Trends Mach. Learn.*, vol. 3, no. 1, pp. 1–122, January 2011.

[18] J.H. Hubbell and S.M. Seltzer, "Radiation and biomolecular physics division, MPL NIST," `https://physics.nist.gov/PhysRefData/XrayMassCoef/tab3.html`.

[19] J. H. Siewerdsen, A. M. Waese, D. J. Moseley, S. Richard, and D. A. Jaffray, "Spektr: A computational tool for X-ray spectral analysis and imaging system optimization," *Medical Physics*, vol. 31, no. 11, pp. 3057–3067, 2004.

[20] W. Xu, F. Xu, M. Jones, B. Keszthelyi, J. Sedat, D. Agard, and K. Mueller, "High-performance iterative electron tomography reconstruction with long-object compensation using graphics processing units (GPUs)," *Journal of structural biology*, 2010.

[21] A. P. Cuadros, C. Peitsch, H. Arguello, and G. R. Arce, "Coded aperture optimization for compressive X-ray tomosynthesis," *Opt. Express*, vol. 23, no. 25, pp. 32788–32802, Dec 2015.

[22] A. P. Cuadros and G. R. Arce, "Coded aperture optimization in compressive X-ray tomography: a gradient descent approach," *Opt. Express*, vol. 25, no. 20, pp. 23833–23849, Oct 2017.